

## Aharonov–Bohm Hamiltonians, isospectrality and minimal partitions

This article has been downloaded from IOPscience. Please scroll down to see the full text article.

2009 J. Phys. A: Math. Theor. 42 185203

(<http://iopscience.iop.org/1751-8121/42/18/185203>)

View [the table of contents for this issue](#), or go to the [journal homepage](#) for more

Download details:

IP Address: 171.66.16.153

The article was downloaded on 03/06/2010 at 07:38

Please note that [terms and conditions apply](#).

# Aharonov–Bohm Hamiltonians, isospectrality and minimal partitions

V Bonnaillie-Noël<sup>1</sup>, B Helffer<sup>2</sup> and T Hoffmann-Ostenhof<sup>3,4</sup>

<sup>1</sup> IRMAR, ENS Cachan Bretagne, Univ. Rennes 1, CNRS, UEB, av Robert Schuman, 35 170 Bruz, France

<sup>2</sup> Laboratoire de Mathématiques, Bat. 425, Univ Paris-Sud and CNRS, 91 405 Orsay Cedex, France

<sup>3</sup> International Erwin Schrödinger Institute for Mathematical Physics, Boltzmannngasse 9, A-090 Wien, Austria

<sup>4</sup> Institut für Theoretische Chemie, Währingerstrasse 17, Universität Wien, A-1090 Vienna, Austria

E-mail: [Virginie.Bonnaillie@bretagne.ens-cachan.fr](mailto:Virginie.Bonnaillie@bretagne.ens-cachan.fr), [Bernard.Helffer@math.u-psud.fr](mailto:Bernard.Helffer@math.u-psud.fr) and [thoffman@esi.ac.at](mailto:thoffman@esi.ac.at)

Received 28 November 2008, in final form 13 March 2009

Published 8 April 2009

Online at [stacks.iop.org/JPhysA/42/185203](http://stacks.iop.org/JPhysA/42/185203)

## Abstract

The spectral analysis of Aharonov–Bohm Hamiltonians with flux  $\frac{1}{2}$  leads surprisingly to a new insight on some questions of isospectrality appearing for example in Jakobson *et al* (2006 *J. Comput. Appl. Math.* **194** 141–55) and Levitin *et al* (*J. Phys. A: Math. Gen.* **39** 2073–82) and of minimal partitions (Helffer *et al* 2009 *Ann. Inst. H. Poincaré Anal. Non Linéaire* **26** 101–38). We will illustrate this point of view by discussing the question of spectral minimal 3-partitions for the rectangle  $]-\frac{a}{2}, \frac{a}{2}[ \times ]-\frac{b}{2}, \frac{b}{2}[$ , with  $0 < a \leq b$ . It has been observed in Helffer *et al* (2009 *Ann. Inst. H. Poincaré Anal. Non Linéaire* **26** 101–38) that when  $0 < \frac{a}{b} < \sqrt{\frac{3}{8}}$  the minimal 3-partition is obtained by the three nodal domains of the third eigenfunction corresponding to the three rectangles  $]-\frac{a}{2}, \frac{a}{2}[ \times ]-\frac{b}{2}, -\frac{b}{6}[$ ,  $]-\frac{a}{2}, \frac{a}{2}[ \times ]-\frac{b}{6}, \frac{b}{6}[$  and  $]-\frac{a}{2}, \frac{a}{2}[ \times ]\frac{b}{6}, \frac{b}{2}[$ . We will describe a possible mechanism of transition for increasing  $\frac{a}{b}$  between these nodal minimal 3-partitions and non-nodal minimal 3-partitions at the value  $\sqrt{\frac{3}{8}}$  and discuss the existence of symmetric candidates for giving minimal 3-partitions when  $\sqrt{\frac{3}{8}} < \frac{a}{b} \leq 1$ . Numerical analysis leads very naturally to nice questions of isospectrality which are solved by the introduction of Aharonov–Bohm Hamiltonians or by going on the double covering of the punctured rectangle.

PACS number: 02.30.Jr

Mathematics Subject Classification: 35B05

### 1. Introduction

In continuation of [19], we have analyzed in [20] the question of minimal 3-partitions for the disc and introduced new tools for this partially successful analysis. In the same spirit, we discuss here the similar question for the rectangle  $\mathbf{R}_{a,b} := ]-\frac{a}{2}, \frac{a}{2}[ \times ]-\frac{b}{2}, \frac{b}{2}[$ , with  $0 < a \leq b$ . For a given partition<sup>5</sup>  $\mathcal{D}$  of an open set  $\Omega$  by  $k$  open subsets  $D_i$ , we can consider

$$\Lambda(\mathcal{D}) = \max_{i=1,\dots,k} \lambda(D_i), \tag{1.1}$$

where  $\lambda(D_i)$  is the ground-state energy of the Dirichlet Laplacian on  $D_i$ . We denote the infimum on every  $k$ -partitions of  $\Omega$  by

$$\mathfrak{L}_k(\Omega) = \inf_{\mathcal{D} \in \Omega_k} \Lambda(\mathcal{D}). \tag{1.2}$$

We look for minimal  $k$ -partitions, that are partitions such that  $\mathfrak{L}_k(\Omega) = \Lambda(\mathcal{D})$ .

It has been observed in [19] that, when  $0 < \frac{a}{b} < \sqrt{\frac{3}{8}}$  the minimal 3-partition is given by the three nodal domains of the third eigenfunction corresponding to the three rectangles  $]-\frac{a}{2}, \frac{a}{2}[ \times ]-\frac{b}{2}, -\frac{b}{6}[$ ,  $]-\frac{a}{2}, \frac{a}{2}[ \times ]-\frac{b}{6}, \frac{b}{6}[$  and  $]-\frac{a}{2}, \frac{a}{2}[ \times ]\frac{b}{6}, \frac{b}{2}[$ .

In the case when  $\sqrt{\frac{3}{8}} < \frac{a}{b} \leq 1$ , we can show as for the disc, see [8], that  $\mathfrak{L}_3(\mathbf{R}_{a,b})$  is not an eigenvalue. Indeed, the second and third eigenvalues  $\lambda_2(\mathbf{R}_{a,b})$  and  $\lambda_3(\mathbf{R}_{a,b})$  correspond to eigenfunctions with two nodal domains and the fourth one satisfies  $\lambda_2(\mathbf{R}_{a,b}) \leq \lambda_3(\mathbf{R}_{a,b}) < \lambda_4(\mathbf{R}_{a,b})$ . By theorem 2.3 below, see [19] for the proof,  $\mathfrak{L}_3(\mathbf{R}_{a,b})$  cannot be an eigenvalue and hence the associated minimal partition cannot be nodal.

We will describe in section 4 a possible mechanism of transition for increasing  $\frac{a}{b}$  between these nodal minimal 3-partitions and non-nodal minimal 3-partitions at the value  $\sqrt{\frac{3}{8}}$  and discuss the existence of symmetric candidates for giving minimal 3-partitions when  $\sqrt{\frac{3}{8}} < \frac{a}{b} \leq 1$  in sections 6 and 7.

We can exhibit numerically some candidates for the minimal 3-partition using symmetry. Assuming that there is a minimal partition which is symmetric with respect to the axis  $\{y = 0\}$ , and intersecting the partition with the half-square  $]-\frac{1}{2}, \frac{1}{2}[ \times ]0, \frac{1}{2}[$ , one is reduced to analyzing a family of Dirichlet–Neumann problems. Numerical computations<sup>6</sup> performed by V Bonnaillie-Noël and G Vial (in January 2006) lead to a natural candidate  $\mathcal{D}$  for a symmetric minimal partition (see figure 1(a)). We observe numerically that the three lines of  $N(\mathcal{D})$  (i.e., the interior boundary of the subdomains  $D_i$  of the partition, see definition (2.4)) meet at the center  $(0, 0)$  of the square. As expected by the theory they meet at this critical point with equal angle  $\frac{2\pi}{3}$  and meet the boundary orthogonally. This choice of symmetry is not unique. By exploring numerically the possibility of a minimal partition with another symmetry (diagonal), we get the surprise of finding another candidate  $\mathcal{D}^{\text{new}}$  with  $\Lambda(\mathcal{D}^{\text{new}}) = \Lambda(\mathcal{D})$  (see figure 1(b)).

This leads very naturally to nice questions of isospectrality which are solved using Aharonov–Bohm Hamiltonians or by going on the double covering of the punctured rectangle. Sections 5 and 6 concern these questions.

This paper is organized as follows:

In section 2, we recall some notation and properties concerning the nodal partitions.

In section 3, we start with the analysis of the rectangle based on the results of [19] and enumerate in particular all the possible Courant-sharp situations. There appears the limiting case  $\frac{a}{b} = \sqrt{\frac{3}{8}}$  detailed in section 4 in which a mechanism is proposed which explains the transition between the nodal 3-partition and the non-nodal one.

<sup>5</sup> See the next section for precise definitions.

<sup>6</sup> See <http://w3.bretagne.ens-cachan.fr/math/simulations/MinimalPartitions/>.

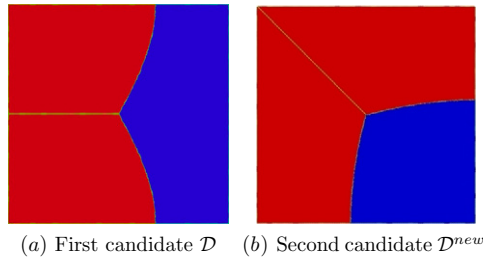


Figure 1. Candidates for the minimal 3-partition of the square.

Motivated by the numerical simulations for the square we find two candidates for the minimal 3-partition with the same energy. We analyze in section 5 the Aharonov–Bohm Hamiltonian and give some isospectral properties for rectangles. This theory is applied in section 6 to explain numerical simulations for the minimal 3-partitions on the square. The paper ends in section 7 with some heuristics on the deformation of symmetric minimal partitions corroborated with numerical simulations for rectangles  $]-\frac{\epsilon\pi}{2}, \frac{\epsilon\pi}{2}[ \times ]-\frac{\pi}{2}, \frac{\pi}{2}[$  from  $\epsilon = \sqrt{\frac{3}{8}}$  to  $\epsilon = 1$ .

Some of the results have been announced in [17].

## 2. Definitions, notation and previous results

As in [19] (see also [20]), we consider the Dirichlet Laplacian on a bounded domain  $\Omega \subset \mathbb{R}^2$ , which is piecewise  $C^\infty$ . We denote, for any open domain  $D$ , the lowest eigenvalue of the Dirichlet realization  $H(D)$  of  $-\Delta$  in  $D$  by  $\lambda(D)$ . For any function  $u \in C_0^0(\overline{\Omega})$ , we introduce

$$N(u) = \overline{\{x \in \Omega \mid u(x) = 0\}} \tag{2.1}$$

and call the components of  $\Omega \setminus N(u)$  the nodal domains of  $u$ . The number of nodal domains of such a function is denoted by  $\mu(u)$ .

We now recall the main definitions and results concerning spectral minimal partitions and refer to [19] for proofs and details. For  $k \geq 1$  ( $k \in \mathbb{N}$ ), we call a  $k$ -partition of  $\Omega$  a family  $\mathcal{D} = \{D_i\}_{i=1}^k$  of pairwise disjoint open domains in  $\Omega$ . Such a partition is called *strong* if

$$\text{Int}(\overline{\bigcup_{i=1}^k D_i}) \setminus \partial\Omega = \Omega. \tag{2.2}$$

We denote by  $\mathfrak{D}_k$  the set of such partitions. Notations (1.1) and (1.2) are now precisely defined.  $\mathcal{D}$  is called a (spectral)<sup>7</sup> minimal  $k$ -partition if  $\mathfrak{L}_k(\Omega) = \Lambda(\mathcal{D})$  and a nodal minimal  $k$ -partition if  $\mathcal{D}$  consists of the nodal domains of an eigenfunction of  $H(\Omega)$ .

To each strong partition  $\mathcal{D}$  we associate a graph  $G(\mathcal{D})$  in the following way:

We say  $D_i, D_j \in \mathcal{D}$  are *neighbors*, and we denote this by  $D_i \sim D_j$ , if

$$\text{Int}(\overline{D_i \cup D_j}) \setminus \partial\Omega \text{ is connected.} \tag{2.3}$$

We associate with each  $D_i \in \mathcal{D}$  a vertex  $v_i$  and for each pair  $D_i \sim D_j$  an edge  $e_{i,j}$ . This defines a planar graph  $G(\mathcal{D})$ . We say that the partition is *admissible* if the corresponding graph is bipartite. We recall that a nodal partition is always admissible.

Attached to a partition  $\mathcal{D}$ , we can associate a closed set  $N \in \overline{\Omega}$  defined by

$$N(\mathcal{D}) = \bigcup_i \overline{(\partial D_i \cap \Omega)}. \tag{2.4}$$

<sup>7</sup> We will omit the word spectral.

This leads us to introduce the set  $\mathcal{M}(\Omega)$  of regular closed sets  $N$ .

**Definition 2.1.** A closed set  $N \subset \overline{\Omega}$  belongs to  $\mathcal{M}(\Omega)$  if  $N$  satisfies the following:

- (i) There are finitely many distinct  $x_i \in \Omega \cap N$  and associated positive integers  $\nu(x_i) \geq 3$  such that, in a sufficiently small neighborhood of each  $x_i$ ,  $N$  is the union of  $\nu(x_i)$  smooth arcs (non-self-crossing) with one end at  $x_i$  and such that in the complement of these points in  $\Omega$ ,  $N$  is locally diffeomorphic to a regular curve. The set of these critical points of  $N$  is denoted by  $X(N)$ .
- (ii)  $\partial\Omega \cap N$  consists of a finite set of points  $z_i$  such that at each  $z_i$ ,  $\rho(z_i)$  arcs hit the boundary with  $\rho(z_i) \geq 1$ . We denote the set of critical points of  $N \cap \partial\Omega$  by  $Y(N)$ .
- (iii)  $N$  has the equal angle meeting property, i.e. the arcs defining  $N \setminus (X(N) \cup Y(N))$  meet with equal angles at each  $x_i \in X(N)$  and also with equal angles at the  $z_i \in Y(N)$ . For the boundary points  $z_i$  we mean that the two arcs in the boundary are included.

Hence the regular sets share with nodal sets all their standard properties except at isolated critical points where they have only<sup>8</sup> the equal angle meeting property.

A partition  $\mathcal{D}$  is called regular if the corresponding  $N(\mathcal{D})$  is regular. Let us now recall the main theorems.

**Theorem 2.2.** For any  $k$  there exists a minimal regular strong  $k$ -partition and any minimal  $k$ -partition admits a representative which is regular and strong.

The existence of a minimal regular strong partition has been shown<sup>9</sup> by Conti–Terracini–Verzini in [13–15], while the second part of the theorem has been shown in [19].

In the following, we always consider the regular representative without mentioning it explicitly. We have now the following converse theorem (see [19]).

**Theorem 2.3.** Assume that there is a minimal admissible  $k$ -partition. Then this partition is associated with the nodal set of an eigenfunction corresponding to  $\mathfrak{L}_k(\Omega)$ .

This result was completed in [19] in relation with the Courant-sharp property. We recall that if  $u$  is an eigenfunction of the Dirichlet Laplacian in  $\Omega$  attached to the  $k$ th eigenvalue  $\lambda_k$ , then Courant’s theorem says that the number of nodal domains  $\mu(u)$  satisfies  $\mu(u) \leq k$ . Pleijel’s theorem says that, when the dimension is  $\geq 2$ , then the previous inequality is strict for  $k$  large.

As in [2], we say that  $u$  is *Courant sharp* if  $\mu(u) = k$ . For any integer  $k \geq 1$ , we denote by  $L_k(\Omega)$  the smallest eigenvalue for which the eigenspace contains an eigenfunction with  $k$  nodal domains. In general we have

$$\lambda_k(\Omega) \leq \mathfrak{L}_k(\Omega) \leq L_k(\Omega). \tag{2.5}$$

The next result of [19] gives the full picture of the equality cases:

**Theorem 2.4.** If  $\mathfrak{L}_k(\Omega) = L_k(\Omega)$  or  $\lambda_k(\Omega) = \mathfrak{L}_k(\Omega)$ , then

$$\lambda_k(\Omega) = \mathfrak{L}_k(\Omega) = L_k(\Omega).$$

In addition, any minimal (regular)  $k$ -partition is a nodal partition corresponding to an eigenfunction associated with  $\lambda_k(\Omega)$ .

As a consequence of Euler’s formula, we have described in [20] the possible topological types of a non-admissible minimal 3-partition of a connected regular open set.

<sup>8</sup> We do no longer assume that the number of lines arriving at a critical point is even.

<sup>9</sup> See also [17] and [12].

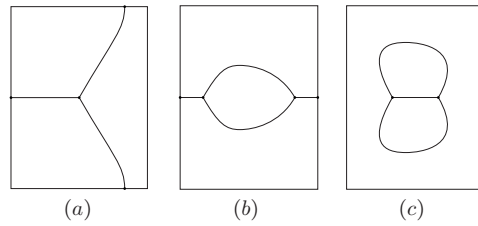


**Figure 2.** The three configurations (a), (b) and (c), with an additional symmetry with respect to the  $x$ -axis.

**Proposition 2.5.** Let  $\Omega$  be simply connected and let us consider a minimal 3-partition  $\mathcal{D} = (D_1, D_2, D_3)$  of  $\Omega$  associated with  $\mathfrak{L}_3(\Omega)$ . Let us suppose that

$$\lambda_3(\Omega) < \mathfrak{L}_3(\Omega). \tag{2.6}$$

For  $N = N(\mathcal{D})$ , we denote by  $v(x_i)$  and  $\rho(z_i)$  the number of arcs associated with  $x_i \in X(N)$ , respectively  $z_i \in Y(N)$ . Then there are three possibilities (see figure 2):

- (a)  $X(N)$  consists of one point  $x$  with  $v(x) = 3$  and  $Y(N)$  consists of either three distinct  $y_1, y_2, y_3$  points with  $\rho(y_1) = \rho(y_2) = \rho(y_3) = 1$ , two distinct points  $y_1, y_2$  with  $\rho(y_1) = 2, \rho(y_2) = 1$  or one point  $y$  with  $\rho(y) = 3$ .
- (b)  $X(N)$  consists of two distinct points  $x_1, x_2$  with  $v(x_1) = v(x_2) = 3$ .  $Y(N)$  consists either of two points  $y_1, y_2$  such that  $\rho(y_1) + \rho(y_2) = 2$  or of one point  $y$  with  $\rho(y) = 2$ .
- (c)  $X(N)$  consists again of two distinct points  $x_1, x_2$  with  $v(x_1) = v(x_2) = 3$ , but  $Y(N) = \emptyset$ .

### 3. A first analysis of the rectangle

This part is taken from [19]. Note that when  $\Omega$  is a rectangle  $\mathbf{R}_{a,b} := ]-\frac{a}{2}, \frac{a}{2}[ \times ]-\frac{b}{2}, \frac{b}{2}[$ , the spectrum of  $H(\mathbf{R}_{a,b})$  and the properties of the eigenfunctions are analyzed as toy models in [24, section 4]. The spectrum is given by

$$\lambda_{m,n} := \pi^2 \left( \frac{m^2}{a^2} + \frac{n^2}{b^2} \right) \quad \text{with} \quad (m, n) \in (\mathbb{N}^*)^2.$$

These eigenvalues are simple if  $a^2/b^2$  is irrational. Except for specific remarks concerning the square or the case when  $a^2/b^2 = 3/8$ , we assume

$$a^2/b^2 \text{ is irrational.} \tag{3.1}$$

So we can associate with each eigenvalue  $\lambda_{m,n}$ , up to a non-zero multiplicative constant, a unique eigenfunction  $u_{m,n}$  such that  $\mu(u_{m,n}) = mn$ . Given  $k \in \mathbb{N}^*$ , the lowest eigenvalue corresponding to  $k$  nodal domains is given, at least under assumption (3.1), by

$$L_k(\mathbf{R}_{a,b}) = \pi^2 \inf_{mn=k} \left( \frac{m^2}{a^2} + \frac{n^2}{b^2} \right). \tag{3.2}$$

In the case when  $a^2/b^2$  is rational we could have problems in the case of multiplicities. We have then to analyze a continuous family of nodal sets of eigenfunctions living in an eigenspace of dimension  $> 1$ . We will see in section 4 that it is just for these values that new nodal partitions

may appear, which could be, by deformation, the starting point of non-admissible minimal partitions.

We now recall all the possible Courant-sharp situations<sup>10</sup> described in [19]:

- (i)  $m = 3, n = 2$  and  $\frac{3}{5} \leq \frac{a^2}{b^2} \leq \frac{5}{8}$ .
- (ii)  $m = 2, n = 2$  and  $\frac{3}{5} \leq \frac{a^2}{b^2} \leq 1$ .
- (iii)  $m = 1, n > 1$  and  $\frac{a^2}{b^2} \leq \frac{3}{n^2-1}$ .

If we now focus on the case  $k = 3$ , we get that  $\lambda_3(\mathbf{R}_{a,b})$  is Courant sharp iff  $a^2/b^2 \leq 3/8$ . Hence, the limiting situation is

$$\frac{a^2}{b^2} = \frac{3}{8}.$$

This corresponds to a double eigenvalue and to the pairs  $(m, n) = (1, 3)$  and  $(m, n) = (2, 1)$ .

#### 4. Transition from Courant-sharp to a non-nodal minimal partition

We start from a rectangle with  $a = \pi\epsilon$  and  $b = \pi$  and would like to analyze  $\mathcal{L}_3(\epsilon) := \mathcal{L}_3(\mathbf{R}_{\pi\epsilon,\pi})$ . The critical situation corresponds to

$$\epsilon = \sqrt{3/8}. \tag{4.1}$$

So the first result (deduced from [19]) which was recalled in the previous section writes:

**Proposition 4.1.**

- (i) If  $\epsilon \leq \sqrt{3/8}$ , then  $\mathcal{L}_3(\epsilon) = 9 + 1/\epsilon^2$  and  $\mathcal{L}_3(\epsilon)$  is an eigenvalue.
- (ii) If  $\sqrt{3/8} < \epsilon \leq 1$ , then  $\mathcal{L}_3(\epsilon) < 9 + 1/\epsilon^2$ .

We would like to understand how the transition occurs at  $\epsilon = \sqrt{3/8}$ . We make the assumption that in the deformation the minimal partition remains symmetric with respect to  $y = 0$ . This is indeed the case for  $\epsilon < \sqrt{3/8}$ , because the eigenfunction corresponding to  $\lambda_{1,3}$  is  $\cos \frac{x}{\epsilon} \cos 3y$  and the corresponding nodal lines are composed of two horizontal lines  $y = -\pi/6$  and  $y = \pi/6$ . This is also the case for  $\epsilon = \sqrt{3/8}$  because all the eigenfunctions have this symmetry and any minimal partition is nodal.

Numerical computations for the rectangles (the case of the square which inherits more symmetries will be analyzed separately) push us to first conjecture that the nodal lines  $N(\mathcal{D})$  for the minimal 3-partition  $\mathcal{D}$  are, for  $\epsilon \in ]\sqrt{3/8}, 1[$ , the union of a segment  $[-\pi/2, x_0(\epsilon)]$  (on the line  $y = 0$ ) and of two symmetric arcs connecting the point  $(x_0(\epsilon), 0)$  to the boundary of the rectangle (up and down).

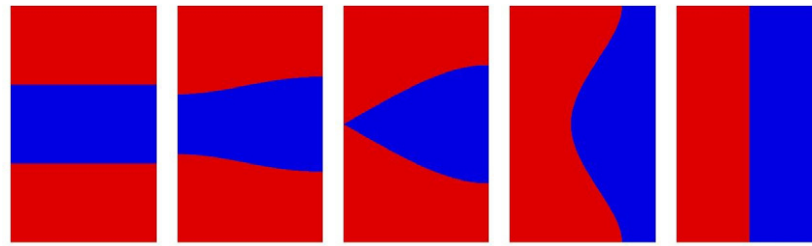
The second conjecture is that  $x_0(\epsilon)$  is increasing monotonically from  $-\pi/2$  to 0 for  $\epsilon \in ]\sqrt{3/8}, 1[$  and that  $\lim_{\epsilon \rightarrow 1} x_0(\epsilon) = 0$ . This has been partially verified (assuming that the reflexion symmetry and that the minimal 3-partition are of type (a)) numerically.

The third conjecture is that the minimal 3-partition will ‘tend’ as  $\epsilon$  tends to  $\sqrt{3/8}$  from above to a nodal partition, losing there its non-bipartite character.

The point here is that, when  $\epsilon = \sqrt{3/8}$ , we have an eigenvalue of multiplicity 2 giving the possibility of constructing a continuous family of nodal minimal 3-partitions. For this, we consider the family

$$\varphi_{\alpha,\beta}(x, y) = \alpha \cos \frac{x}{\epsilon} \cos 3y + \beta \sin \frac{2x}{\epsilon} \cos y,$$

<sup>10</sup> We do not know whether for certain  $a^2/b^2$  rational additional Courant-sharp eigenvalues could show up.



(a)  $\alpha = 1, \beta = 0$  (b)  $\alpha = 5, \beta = 1$  (c)  $\alpha = 2, \beta = 1$  (d)  $\alpha = 1, \beta = 2$  (e)  $\alpha = 0, \beta = 1$

**Figure 3.** Nodal sets of  $\varphi_{\alpha,\beta}(x, y) = \alpha \cos \frac{x}{\epsilon} \cos 3y + \beta \sin \frac{2x}{\epsilon} \cos y$ .

with  $\alpha^2 + \beta^2 \neq 0$ , and analyze its zero set. Of course, for  $t \neq 0$ ,  $\varphi_{\alpha,\beta}$  and  $\varphi_{t\alpha,t\beta}$  have the same zero set.

We first show that the zero set of  $\varphi_{\alpha,\beta}$  has no critical point inside the rectangle for the critical value of  $\epsilon$ . Using the factorization of  $\varphi_{\alpha,\beta}$  in the form

$$\varphi_{\alpha,\beta}(x, y) = \cos y \cos \frac{x}{\epsilon} \left( \alpha(1 - 4 \sin^2 y) + 2\beta \sin \frac{x}{\epsilon} \right),$$

we observe that  $\varphi_{\alpha,\beta} = 0$  is equivalent inside the rectangle to  $\psi_{\alpha,\beta} = 0$  with

$$\psi_{\alpha,\beta}(x, y) := \alpha(1 - 4 \sin^2 y) + 2\beta \sin \frac{x}{\epsilon}. \tag{4.2}$$

Hence we now look at the (closure of the) zero set of  $\psi_{\alpha,\beta}$  in the rectangle and particularly to the critical points inside and at the boundary. If we look at the zeros of  $\partial_x \psi_{\alpha,\beta}$ , we obtain

$$\beta \cos \frac{x}{\epsilon} = 0.$$

This implies  $\beta = 0$  and we get that  $\varphi_{\alpha,0}(x, y) = \alpha \cos 3y \cos \frac{x}{\epsilon}$ . Hence we get that, for any  $(\alpha, \beta) \neq (0, 0)$ , there is no critical point inside this rectangle.

It remains to look at what is going on at the boundary and to determine the singular points where two lines touch. An analysis of the function  $(x, y) \mapsto \alpha(1 - 4 \sin^2 y) + 2\beta \sin \frac{x}{\epsilon}$  at the boundary shows that critical points at the boundary can only occur for  $y = 0$  and  $\alpha \pm 2\beta = 0$ .

Hence we have obtained that the only nodal sets having critical sets are (up to a multiplicative constant) the nodal domains of the eigenfunctions  $\varphi_{2,1}$  and  $\varphi_{2,-1}$ .

Figure 3 gives the nodal set of the functions  $\varphi_{\alpha,\beta}$  for several values of  $(\alpha, \beta)$ .

### 5. Aharonov–Bohm Hamiltonian and isospectrality

As explained in the introduction, this new analysis is motivated by numerical computations showing that pushing the same idea as in [8] but using the symmetry with respect to the diagonal, one gets the same eigenvalue and again a 3-partition with unique singular point at the center. This will be further explained in more detail in subsection 6.1.

**Remark 5.1.** Note that theorem 2.4 implies that for  $\epsilon = \sqrt{3/8}$ , all the minimal 3-partitions are nodal. Hence we have effectively described all the minimal 3-partitions.

#### 5.1. Basic material

This material appears already in [18] and is motivated by the work of Berger–Rubinstein [7]. If  $\Omega$  is an open set such that  $0 \in \Omega$ , a possibility is to consider the Aharonov–Bohm



Laplacian in the punctured  $\dot{\Omega} = \Omega \setminus \{0\}$ , with the singularity of the potential at the center and the normalized flux  $\Phi = 1/2$ . The magnetic potential with flux  $\Phi$  takes the form

$$\mathbf{A}(x, y) = (A_1(x, y), A_2(x, y)) = \Phi \left( -\frac{y}{r^2}, \frac{x}{r^2} \right). \quad (5.1)$$

We know that the magnetic field vanishes identically in  $\dot{\Omega}$  and, in any cut domain (such that it becomes simply connected), one has

$$A_1 dx + A_2 dy = \Phi d\theta, \quad (5.2)$$

where

$$z = x + iy = r e^{i\theta}. \quad (5.3)$$

So the Aharonov–Bohm operator in any open set  $\dot{\Omega} \subset \mathbb{R}^2 \setminus \{0\}$  will always be defined by considering the Friedrichs extension starting from  $C_0^\infty(\dot{\Omega})$  and the associated differential operator is

$$-\Delta_{\mathbf{A}} := (D_x - A_1)^2 + (D_y - A_2)^2. \quad (5.4)$$

From now on, we will assume that

$$\Phi = \frac{1}{2}. \quad (5.5)$$

In polar coordinates (which of course are not very well adapted to the square but permit a good analysis at the origin), the Aharonov–Bohm Laplacian reads

$$-\Delta_{\mathbf{A}} = \left( D_x + \frac{1}{2} \frac{\sin \theta}{r} \right)^2 + \left( D_y - \frac{1}{2} \frac{\cos \theta}{r} \right)^2, \quad (5.6)$$

or

$$-\Delta_{\mathbf{A}} = -\frac{\partial^2}{\partial r^2} - \frac{1}{r} \frac{\partial}{\partial r} + \frac{1}{r^2} \left( i\partial_\theta + \frac{1}{2} \right)^2. \quad (5.7)$$

This operator preserves ‘real’ functions in some modified sense. Following [18], we will say that a function  $u$  is  $K$ -real, if it satisfies

$$Ku = u, \quad (5.8)$$

where  $K$  is an antilinear operator in the form

$$K = e^{i\theta} \Gamma, \quad (5.9)$$

and where  $\Gamma$  is the complex conjugation

$$\Gamma u = \bar{u}. \quad (5.10)$$

The fact that  $-\Delta_{\mathbf{A}}$  preserves  $K$ -real eigenfunctions is an immediate consequence of

$$K \circ (-\Delta_{\mathbf{A}}) = (-\Delta_{\mathbf{A}}) \circ K. \quad (5.11)$$

**Remark 5.2.** Note that our choice of  $K$  is not unique.  $K_\alpha = e^{i\alpha} K$  is also antilinear, satisfies (5.11) and

$$K_\alpha^2 = Id.$$

As observed in [18], it is easy to find a basis of  $K$ -real eigenfunctions. These eigenfunctions (which can be identified with real antisymmetric eigenfunctions of the Laplacian on a suitable double covering  $\dot{\Omega}^{\mathcal{R}}$  of  $\dot{\Omega}$ ) have a nice nodal structure (which is locally in the covering the same as the nodal set of real eigenfunctions of the Laplacian), with the specific property that the number of lines in  $\dot{\Omega}$  ending at the origin is odd. More generally a path of index 1 around the origin should always meets an odd number of nodal lines.

5.2. *Symmetries of the rectangle*

We consider now a domain  $\hat{\Omega}$  which has the symmetries of a rectangle. More precisely, if we denote by  $\sigma_1$  and  $\sigma_2$  the symmetries respectively defined by

$$\sigma_1(x, y) = (-x, y), \quad \sigma_2(x, y) = (x, -y), \tag{5.12}$$

we assume that

$$\sigma_1\hat{\Omega} = \hat{\Omega}, \quad \sigma_2\hat{\Omega} = \hat{\Omega}. \tag{5.13}$$

For simplicity, we assume that  $\Omega$  is convex and write

$$\Omega \cap \{y = 0\} = \left] -\frac{a}{2}, \frac{a}{2} \right[ \times \{0\},$$

and

$$\Omega \cap \{x = 0\} = \{0\} \times \left] -\frac{b}{2}, \frac{b}{2} \right[.$$

If  $\Sigma_1$  is the natural action on  $L^2(\hat{\Omega})$  associated with  $\sigma_1$

$$\Sigma_1 u(x, y) = u(-x, y), \tag{5.14}$$

we observe that the Aharonov–Bohm operator does not commute with  $\Sigma_1$  but with the antilinear operator

$$\Sigma_1^c := i\Gamma\Sigma_1. \tag{5.15}$$

So if  $u$  is an eigenfunction,  $\Sigma_1^c u$  is an eigenfunction.

Moreover, and this explains the choice of ‘i’ before  $\Gamma\Sigma_1$ , since  $K$  and  $\Sigma_1^c$  commute,

$$K \circ \Sigma_1^c = \Sigma_1^c \circ K, \tag{5.16}$$

$\Sigma_1^c u$  is also a  $K$ -real eigenfunction if  $u$  is a  $K$ -real eigenfunction. One can do the same thing with  $\Sigma_2$ , associated with  $\sigma_2$ ,

$$\Sigma_2 u(x, y) = u(x, -y). \tag{5.17}$$

This leads this time to

$$\Sigma_2^c = \Gamma\Sigma_2. \tag{5.18}$$

Similarly, we have

$$K \circ \Sigma_2^c = \Sigma_2^c \circ K, \tag{5.19}$$

hence if  $u$  is a  $K$ -real function,  $\Sigma_2^c u$  is also a  $K$ -real eigenfunction.

We now show the following proposition.

**Proposition 5.3.** *If  $\hat{\Omega}$  has the symmetries of the rectangle (5.12), then the multiplicity of the ground-state energy of  $-\Delta_A$  is 2.*

*Actually the multiplicity of any eigenvalue of  $-\Delta_A$  is even.*

**Proof.** As observed in [18], we can reduce the analysis of the Aharonov–Bohm Hamiltonian to the  $K$ -real space  $L_K^2$  where

$$L_K^2(\hat{\Omega}) = \{u \in L^2(\hat{\Omega}), Ku = u\}.$$

The scalar product on  $L_K^2$ , making of  $L_K^2$  a real Hilbert space, is obtained by restricting the scalar product on  $L^2(\hat{\Omega})$  to  $L_K^2$  and it is immediate to verify that  $\langle u, v \rangle$  is indeed real for  $u$  and  $v$  in  $L_K^2$ .

Observing now that

$$\Sigma_1^c \circ \Sigma_1^c = I, \tag{5.20}$$

we obtain by writing

$$u = \frac{1}{2}(I + \Sigma_1^c)u + \frac{1}{2}(I - \Sigma_1^c)u,$$

an orthogonal decomposition of  $L_K^2$  into

$$L_K^2 = L_{K,\Sigma_1}^2 \oplus L_{K,a\Sigma_1}^2, \tag{5.21}$$

where

$$L_{K,\Sigma_1}^2 = \{u \in L_K^2, \Sigma_1^c u = u\},$$

and

$$L_{K,a\Sigma_1}^2 = \{u \in L_K^2, \Sigma_1^c u = -u\}.$$

We have just to show that the restriction  $\Pi_1$  of  $\frac{1}{2}(I + \Sigma_1^c)$  to  $L_K^2$

$$\Pi_1 := \frac{1}{2}(I + \Sigma_1^c)_{/L_K^2}, \tag{5.22}$$

is a projector. It is indeed clear that  $\Pi_1$  is ( $\mathbb{R}$ -)linear and that  $\Pi_1^2 = \Pi_1$ . It remains to verify that  $\Pi_1^* = \Pi_1$ . But we have, for  $u, v$  in  $L_K^2$ ,

$$\langle \Sigma_1^c u, v \rangle = i \langle \Gamma v, \Sigma_1 u \rangle = i \langle \Gamma \Sigma_1 v, u \rangle = \langle \Sigma_1^c v, u \rangle = \langle u, \Sigma_1^c v \rangle.$$

Moreover the decomposition (5.21) is respected by  $-\Delta_A$ .

Similarly, one can define the projector  $\Pi_2$  by restriction of  $\Sigma_2^c$  to  $L_K^2$ .

The second statement of Proposition 5.3 will be a consequence of the following lemma □

**Lemma 5.4.** *Let*

$$\Sigma_3^c = \Sigma_1^c \Sigma_2^c, \tag{5.23}$$

*then  $\Sigma_3^c$  commutes with  $-\Delta_A$  and  $\Pi_3 := (\Sigma_3^c)_{/L_K^2}$  is a unitary operator from  $L_{K,\Sigma_1}^2$  onto  $L_{K,a\Sigma_1}^2$ .*

**Proof.** We note that

$$\Sigma_3^c = i \Sigma_3, \tag{5.24}$$

where  $\Sigma_3$  is associated with

$$\sigma_3(x, y) = (-x, -y). \tag{5.25}$$

The lemma follows then from the property that if  $u$  is a solution of  $Ku = u$  and  $\Sigma_1^c u = u$ , then

$$\Sigma_1^c \Sigma_3^c u = \Sigma_1^c \Sigma_1^c \Sigma_2^c u = -\Sigma_1^c \Sigma_2^c \Sigma_1^c u = -\Sigma_3^c u,$$

where we have used the anticommutation of  $\Sigma_1^c$  and  $\Sigma_2^c$ :

$$\Sigma_1^c \Sigma_2^c = -\Sigma_2^c \Sigma_1^c. \tag{5.26}$$

□

It remains to show that the first eigenvalue has multiplicity 2. We already know that it has an even multiplicity. It is enough to prove that the multiplicity is at most 2. Here we can use the results of [18]. Actually those results have to be extended slightly<sup>11</sup> since they are obtained

<sup>11</sup> The paper of Alziary–Fleckinger–Takac [1] deals with this case.

assuming that the domain is homeomorphic to an annulus (so we are in a limiting case). It has been shown in [18] that the nodal set of a  $K$ -real ground-state is a line joining the center to the outer boundary. If the multiplicity of the ground-state eigenvalue is strictly greater than 2 we can, as in [18], construct by linear combination of eigenfunctions a ground-state for which the zero set hits the outer boundary at two distinct points, hence a contradiction.

We observe that the proof of the proposition gives more explicitly the decomposition of  $-\Delta_A$  on  $L^2_K$  into the direct orthogonal sum of two unitary equivalent Hamiltonians. What we have done with  $\Sigma_1^c$  can similarly be done with  $\Sigma_2^c$ . This gives immediately the following proposition.

**Proposition 5.5.** *The four following operators  $-\Delta_{A,\Sigma_1}$ ,  $-\Delta_{A,a\Sigma_1}$ ,  $-\Delta_{A,\Sigma_2}$  and  $-\Delta_{A,a\Sigma_2}$  respectively defined by the restriction of  $-\Delta_A$  to  $L^2_{K,\Sigma_1}$ ,  $L^2_{K,a\Sigma_1}$ ,  $L^2_{K,\Sigma_2}$  and  $L^2_{K,a\Sigma_2}$  are isospectral to  $-\Delta_A$ . Moreover  $\lambda$  is an eigenvalue of any of the first four operators with multiplicity  $k(\lambda)$  if and only if  $\lambda$  is an eigenvalue of multiplicity  $2k(\lambda)$  of  $-\Delta_A$ .*

Now we would like to analyze the nodal patterns of eigenfunctions in the various symmetry spaces.

**Lemma 5.6.** *If  $u \in C^\infty(\dot{\Omega}) \cap L^2_{K,\Sigma_2}$  then its nodal set contains  $[-\frac{a}{2}, 0] \times \{0\}$ . Moreover, in  $\dot{\Omega} \setminus \{-\frac{a}{2}, 0\} \times \{0\}$ ,*

$$v = e^{-i\frac{\theta}{2}}u \quad (\text{with } \theta \in (-\pi, \pi))$$

satisfies

$$\Gamma v = v \quad \text{and} \quad \Sigma_2 v = v.$$

**Proof.** Noting that  $Ku = u$  and  $\Sigma_2^c u = u$  for  $y = 0$  and  $x < 0$  we immediately obtain that  $\bar{u}(x, 0) = u(x, 0) = -\bar{u}(x, 0)$ . Hence  $u(x, 0) = 0$  for  $x < 0$ .

An immediate computation gives

$$\Gamma v = e^{i\frac{\theta}{2}}\Gamma u = e^{-i\frac{\theta}{2}}Ku = e^{-i\frac{\theta}{2}}u = v,$$

and

$$\Sigma_2 v = e^{i\frac{\theta}{2}}\Sigma_2 u = e^{i\frac{\theta}{2}}\Gamma u = v. \quad \square$$

We would like to compare some Dirichlet–Neumann problems on half-domains. We call upper-half- $\Omega$  the set

$$\Omega^{\text{uh}} = \Omega \cap \{y > 0\}, \tag{5.27}$$

and introduce similarly the lower-half, left-half and right-half domains defined by

$$\Omega^{\text{lh}} = \Omega \cap \{y < 0\}, \quad \Omega^{\text{leh}} = \Omega \cap \{x < 0\}, \quad \Omega^{\text{rth}} = \Omega \cap \{x > 0\}. \tag{5.28}$$

The previous lemma leads to the following proposition.

**Proposition 5.7.** *If  $u$  is a  $K$ -real  $\Sigma_2^c$  invariant eigenfunction of  $-\Delta_A$ , then the restriction to  $\Omega^{\text{uh}}$  of  $e^{-i\frac{\theta}{2}}u$  (with  $\theta \in (-\pi, +\pi)$ ) is a real eigenfunction of the realization of the Laplacian in  $\Omega^{\text{uh}}$ , with the following Dirichlet–Neumann condition at  $\partial\Omega^{\text{uh}}$ : Dirichlet except on  $]0, \frac{a}{2}] \times \{0\}$  where we put Neumann.*

*In particular, if  $\lambda$  is an eigenvalue of  $-\Delta_A$ , then  $\lambda$  is an eigenvalue of the Laplacian in  $\Omega^{\text{uh}}$  with this Dirichlet–Neumann condition.*

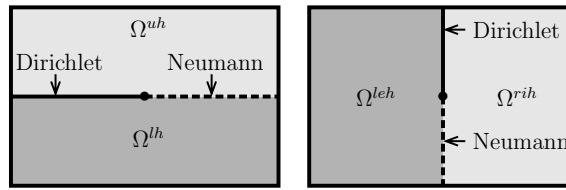


Figure 4. Domains  $\Omega^{uh}$ ,  $\Omega^{lh}$ ,  $\Omega^{leh}$ ,  $\Omega^{rih}$ .

Conversely, if we consider an eigenfunction  $u$  of the Laplacian in  $\Omega^{uh}$  with this Dirichlet–Neumann condition and extend it into a  $\Sigma_2$ -symmetric function  $u^{ext}$  in  $\Omega \setminus \{]-\frac{a}{2}, 0] \times \{0\}\}$ , then

$$v = e^{i\frac{\theta}{2}} u^{ext} \tag{5.29}$$

is a  $K$ -real eigenfunction of the Aharonov–Bohm Laplacian. More precisely, the function  $v$  is first defined by formula (5.29) for  $\theta \in ]-\pi, \pi[$  and then extended as a  $L^2$  function on  $\hat{\Omega}$ . Due to the properties of  $u$ , one can verify that  $v$  is in the form domain of the Aharonov–Bohm operator. Starting from a ground-state of the  $DN$ -problem in  $\Omega^{uh}$ , we get a  $K$ -real eigenstate in  $L^2_{K, \Sigma_2}$  of the Aharonov–Bohm operator.

Similarly, we have the following proposition.

**Proposition 5.8.** *If  $u$  is a  $K$ -real  $\Sigma_1^c$  antisymmetric eigenfunction of  $-\Delta_A$ , then the restriction to  $\Omega^{rih}$  of  $e^{-i\frac{\theta}{2}} u$  (with  $\theta \in ]-\frac{3\pi}{2}, \frac{\pi}{2}[$ ) is a real eigenfunction of the realization of the Laplacian in  $\Omega^{rih}$ , with the following Dirichlet–Neumann condition at  $\partial\Omega^{rih}$ : Dirichlet except on  $\{0\} \times ]-\frac{b}{2}, 0[$  where we put Neumann.*

*In particular, if  $\lambda$  is an eigenvalue of  $-\Delta_A$ , then  $\lambda$  is an eigenvalue of the Laplacian in  $\Omega^{rih}$  with this Dirichlet–Neumann condition.*

Conversely, if we consider an eigenfunction  $u$  of the Laplacian in  $\Omega^{rih}$  with this Dirichlet–Neumann condition and extend it into a  $\Sigma_1$ -symmetric function  $u^{ext}$  in  $\Omega \setminus \{(0) \times ]0, \frac{b}{2}[ \}$ , then

$$v = e^{i\frac{\theta}{2}} u^{ext} \tag{5.30}$$

is a  $K$ -real eigenfunction of the Aharonov–Bohm Laplacian, which is antisymmetric with respect to  $\Sigma_1^c$ . More precisely, the function  $v$  is first defined by formula (5.30) for  $\theta \in ]-\frac{3\pi}{2}, \frac{\pi}{2}[$  and then extended as a  $L^2$  function on  $\hat{\Omega}$ .

Using in addition lemma 5.4 and obvious unitary equivalences by  $\Sigma_1$  and  $\Sigma_2$ , we obtain the following result.

**Proposition 5.9.** *The following problems have the same eigenvalues:*

- *The Dirichlet problem for the Aharonov–Bohm operator on  $\hat{\Omega}$ .*
- *The Dirichlet–Neumann problem for the Laplacian on  $\Omega^{uh}$ .*
- *The Dirichlet–Neumann problem for the Laplacian on  $\Omega^{leh}$ .*
- *The Dirichlet–Neumann problem for the Laplacian on  $\Omega^{lh}$ .*
- *The Dirichlet–Neumann problem for the Laplacian on  $\Omega^{rih}$ .*

Of course this applies in particular to the case of the rectangle.

Let us go a little further by giving explicitly an intertwining unitary operator from  $L^2_{K, \Sigma_1}$  onto  $L^2_{K, \Sigma_2}$  proving the isospectrality. This is the object of the following lemma.

**Lemma 5.10.** *The operator*

$$U_{21} := \frac{1}{\sqrt{2}}(I + \Sigma_2^c)$$

*is a unitary operator from  $L^2_{K,\Sigma_1}$  onto  $L^2_{K,\Sigma_2}$ . Its inverse is given by*

$$U_{12} := \frac{1}{\sqrt{2}}(I + \Sigma_1^c).$$

**Proof.** Let  $u \in L^2_{K,\Sigma_1}$ , then, using (5.26),

$$U_{12}U_{21}u = \frac{1}{2}(I + \Sigma_1^c + \Sigma_2^c + \Sigma_1^c\Sigma_2^c)u = \frac{1}{2}(I + \Sigma_1^c + \Sigma_2^c - \Sigma_2^c\Sigma_1^c)u = u.$$

The proof that  $U_{21}U_{12} = I$  on  $L^2_{K,\Sigma_2}$  is obtained in the same way. Let us prove that the norm is conserved. If  $u \in L^2_{K,\Sigma_1}$ , then

$$\|U_{21}u\|^2 = \|u\|^2 + \frac{1}{2}\langle \Sigma_2^c u, u \rangle + \frac{1}{2}\langle u, \Sigma_2^c u \rangle.$$

But if  $\Sigma_1^c u = u$ , we can write

$$\begin{aligned} \langle u, \Sigma_2^c u \rangle &= \langle u, \Sigma_2^c \Sigma_1^c u \rangle \\ &= i \langle u, \Sigma_2 \Sigma_1 u \rangle \\ &= i \langle \Sigma_2 \Sigma_1 u, u \rangle \\ &= -\langle \Sigma_2^c u, \Sigma_1^c u \rangle \\ &= -\langle \Sigma_2^c u, u \rangle. \end{aligned}$$

This leads to

$$\|U_{21}u\|^2 = \|u\|^2, \quad \forall u \in L^2_{K,\Sigma_1}. \tag{5.31}$$

□

We can now explicitly write the intertwining unitary operator between the Dirichlet Neumann problem for the Laplacian on  $\Omega^{\text{uh}}$  and the Dirichlet Neumann problem on  $\Omega^{\text{rth}}$ . This is the composition of the extension (5.29), the unitary transformation  $U_{21}$ , the operator  $\Sigma_3^c$ , the multiplication by  $e^{-i\frac{\theta}{2}}$  and the restriction to  $\Omega^{\text{rth}}$ .

## 6. Application to minimal 3-partitions

### 6.1. Discussion on the square

We look at the first excited eigenvalue of the Dirichlet problem in the punctured square. The rules of [18] give constraints about the nodal structure of the  $K$ -real eigenfunctions, which were already used (for example in the proof of proposition 5.3). In particular we have an odd number of lines arriving at the center. So it is clear that  $\{0\}$  belongs to the nodal set. If three lines arrive at 0 and if the nodal partition is a 3-partition of type (a), this gives us a reasonable candidate for the minimal 3-partition.

Let us explain the numerical strategy developed in [8, section 3] to exhibit a candidate for the minimal 3-partition of the square. According to theorem 2.3, if the minimal 3-partition of the square is admissible, it is associated with the nodal set of an eigenfunction for  $\lambda_3$ . But there is no such function and therefore the minimal 3-partition is non-bipartite. Then we look for non-bipartite 3-partitions whose topologies are described in proposition 2.5 and illustrated by figure 2. We first use the axial symmetry along the axis  $\{y = 0\}$ . To recover a partition of type (a), (b) or (c), we compute the second eigenfunction and the next ones of the mixed

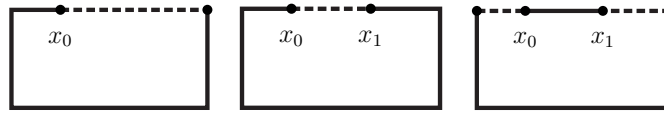


Figure 5. Mixed problems with Dirichlet–Neumann conditions.

Dirichlet–Neumann Laplacian in  $\Omega^{\text{lh}}$  with Dirichlet conditions except respectively on

- $[x_0, a/2] \times \{0\}$  for type (a);
- $[x_0, x_1] \times \{0\}$  for type (b);
- $[-a/2, x_0] \times \{0\} \cup [x_1, a/2] \times \{0\}$  for type (c).

These boundary conditions are illustrated in figure 5. We move the points  $x_0$  and  $x_1$  along the segment  $[-a/2, a/2] \times \{0\}$ . We expect to find an eigenfunction such that, after symmetrization, its associated nodal sets constitute a 3-partition and the nodal lines meet at the interior critical point with an angle of  $2\pi/3$ .

We recall the guess which appears natural in view of the numerical computations. When minimizing over Dirichlet–Neumann problems in  $\Omega^{\text{lh}}$  (by putting Dirichlet except Neumann on  $]x_0, \frac{a}{2}] \times \{0\}$ ), one observes that the minimal second eigenvalue (as a function of  $x_0$ ) such that the two nodal domains give rise by symmetry to a 3-partition is obtained for  $x_0 = 0$ .

Doing the same computation on the diagonal, we observe also numerically that the minimal second eigenvalue (as a function of the point on the diagonal) such that the two nodal domains give rise by symmetry to a three partition is obtained at the center.

Admitting these two numerical results, what we have proved for the square is that the two minimal second eigenvalues are equal.

This could also suggest that we have a continuum of minimal 3-partitions.

This point is not completely clear but could result of the analysis of the singularity at  $\{0\}$ .

When minimizing over Dirichlet–Neumann–Dirichlet or Neumann–Dirichlet–Neumann problems in  $\Omega^{\text{lh}}$ , the numerical computations (see [8, section 3.3]) suggest that the nodal sets of the second eigenfunction never create a 2-partition of  $\Omega^{\text{lh}}$  leading by symmetry to a 3-partition of  $\Omega$ . The corresponding eigenmodes lead to a too high energy; hence do not qualify as possible candidates for minimal 3-partitions.

**Remark 6.1.** Note that we assumed that the minimal partition is symmetric with respect to an axis of symmetry; the numerical experiments make this assumption plausible. One cannot *a priori* exclude that the first excited  $K$ -real eigenfunction of the Aharonov–Bohm Hamiltonian consists of one line joining 0 to  $\partial\Omega$  and the another line joining in  $\tilde{\Omega}$  two points of  $\partial\Omega$ .

### 6.2. The symmetries of the square

We now consider a convex domain which in addition to the invariance by  $\sigma_1$  and  $\sigma_2$  has an invariance by rotation (centered at the origin)  $r_{\frac{\pi}{2}}$  of  $\frac{\pi}{2}$ . We have typically in mind the case of the square. This rotation can be quantized by

$$\mathcal{R}_{\frac{\pi}{2}} u(\cdot) = u(r_{-\frac{\pi}{2}} \cdot), \tag{6.1}$$

where  $r_\alpha$  is the rotation by  $\alpha$  in the plane. We observe from (5.7) that this rotation commutes with the operator:

$$\Delta_A \mathcal{R}_{\frac{\pi}{2}} = \mathcal{R}_{\frac{\pi}{2}} \Delta_A \tag{6.2}$$

(and with its Dirichlet realization in  $\tilde{\Omega}$ ).

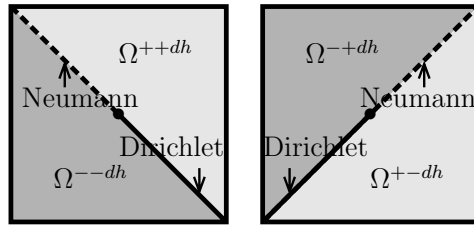


Figure 6. Domains  $\Omega^{--dh}$ ,  $\Omega^{++dh}$ ,  $\Omega^{-+dh}$ ,  $\Omega^{+-dh}$ .

More generally, we have the following lemma.

**Lemma 6.2.** *If  $u$  is a  $K$ -real eigenfunction of the Aharonov–Bohm Hamiltonian on the square, then  $u$  and  $e^{i\frac{\pi}{4}}\mathcal{R}_{\frac{\pi}{2}}u$  are linearly independent  $K$ -real eigenfunctions.*

**Proof.** Let us first verify the  $K$ -reality.

We note that

$$\mathcal{R}_{\frac{\pi}{2}}Kv = \mathcal{R}_{\frac{\pi}{2}}e^{i\theta}\Gamma v = e^{-i\frac{\pi}{2}}e^{i\theta}\Gamma\mathcal{R}_{\frac{\pi}{2}}v,$$

hence

$$\mathcal{R}_{\frac{\pi}{2}}K = e^{-i\frac{\pi}{2}}K\mathcal{R}_{\frac{\pi}{2}}.$$

This can be rewritten in the form

$$(e^{i\frac{\pi}{4}}\mathcal{R}_{\frac{\pi}{2}}) \circ K = K \circ (e^{i\frac{\pi}{4}}\mathcal{R}_{\frac{\pi}{2}}). \tag{6.3}$$

This proves the first statement.

We now show that  $e^{i\frac{\pi}{4}}\mathcal{R}_{\frac{\pi}{2}}u$  and  $u$  are linearly independent (over  $\mathbb{R}$ ) inside the real space  $L^2_K$ . Let us look at the points of the nodal set belonging to the exterior boundary. Their cardinality should be odd by a result of [18] on  $K$ -real eigenfunctions. If  $u$  and  $e^{i\frac{\pi}{4}}\mathcal{R}_{\frac{\pi}{2}}u$  were proportional, this subset is invariant by rotation of  $\frac{\pi}{2}$  and has consequently an even cardinality. This contradicts the previous state.  $\square$

**Proposition 6.3.** *In the case of a convex domain having the symmetries of the square, the Dirichlet–Neumann problem for the Laplacian on the four half-domains respectively defined by*

$$\begin{aligned} \Omega^{--dh} &= \Omega \cap \{x + y < 0\}, & \Omega^{++dh} &= \Omega \cap \{x + y > 0\}, \\ \Omega^{+-dh} &= \Omega \cap \{x - y > 0\}, & \Omega^{-+dh} &= \Omega \cap \{x - y < 0\}, \end{aligned} \tag{6.4}$$

are also isospectral to the problems introduced in proposition 5.5.

**Proof.** We explain below how to get the proposition. We start from  $v \in L^2_{K,\Sigma_2}$ . Let us now consider

$$w = v + e^{i\frac{\pi}{4}}\mathcal{R}_{\frac{\pi}{2}}v.$$

We have already shown that  $w$  is not zero and hence is an eigenfunction. It remains to analyze its zero set which should contain an half-diagonal.

Let us introduce

$$\Sigma_4^c = e^{i\frac{\pi}{4}}\mathcal{R}_{\frac{\pi}{2}}\Sigma_2^c.$$



Using the property that

$$\mathcal{R}_{\frac{\pi}{2}} \Sigma_2^c = \Sigma_2^c \mathcal{R}_{-\frac{\pi}{2}},$$

we can verify that

$$\Sigma_4^c w = w, \quad K w = w. \tag{6.5}$$

For  $\theta = -\frac{3\pi}{4}$  and  $x + iy = re^{i\theta}$ , we obtain

$$\overline{w} e^{i\frac{\pi}{4}} = w, \quad e^{-i\frac{3\pi}{4}} \overline{w} = w,$$

hence  $w = 0$  for  $\theta = -\frac{3\pi}{4}$ . So the restriction of  $w$  to  $\Omega^{-+\text{dh}}$  multiplied by a phase factor leads to an eigenfunction of the DN-problem for the Laplacian in  $\Omega^{-+\text{dh}}$ .

The converse does not introduce new problems. □

### 6.3. The covering approach

As in [19], we can also rewrite all the proofs by lifting the problem on the double covering  $\dot{\Omega}^{\mathcal{R}}$ , using the correspondence between  $L_K^2$  and the real subspace of the functions in  $L^2(\dot{\Omega}^{\mathcal{R}})$  such that  $\Sigma u = -u$  where  $\Sigma$  is associated with the map  $\sigma$  by  $(\Sigma u)(\omega) = u(\sigma(\omega))$ . We recall with the notation of [20] that  $\sigma$  is defined by associating with each point  $\omega$  of  $\dot{\Omega}^{\mathcal{R}}$  the other point  $\sigma(\omega)$  of  $\dot{\Omega}^{\mathcal{R}}$  which has the same projection on  $\dot{\Omega}$ . Our initial proof was actually written in this way but we prefer to present in this paper another point of view.

In a recent paper, Jakobson, Levitin, Nadirashvili, Polterovich [22] obtain also nice isospectrality results involving Dirichlet–Neumann problems. They actually propose three different proofs of their isospectrality results. The second one is a double covering argument which is quite close to what we mentioned in the previous paragraph. But there is no magnetic version and our magnetic examples seem to be new. So it would be interesting to see whether the magnetic approach can produce some isospectrality result which differs from the class of results in this paper and the papers by Levitin, Parnovski and Polterovich [23] or [25].

One should also mention that for these questions of isospectrality a covering argument was already presented in earlier works of Bérard [3–5], Bérard–Besson [6], Sunada [26].

## 7. Some heuristics on the deformation of symmetric minimal partitions and numerical computations

### 7.1. Some heuristics

Here we discuss very heuristically in which general context the numerical computations for the family of rectangles can be done.

One might investigate the special situation where tight upper and lower bounds to  $\mathfrak{L}_3$  are available. We recall from (2.5) that

$$\lambda_k \leq \mathfrak{L}_k \leq L_k.$$

If we have a family of domains depending analytically on a parameter  $\alpha$ ,  $\Omega(\alpha)$ , such that for some  $k$ ,

$$\lim_{\alpha \downarrow 0} \lambda_k(\alpha) = L_k(0) \quad \text{and} \quad \lambda_k(\alpha) < L_k(\alpha) \quad \text{for} \quad \alpha > 0, \tag{7.1}$$

then we are led to the question how a minimal  $k$ -partition of  $\mathfrak{D}_k(\alpha)$  of  $\Omega(\alpha)$  behaves as  $\alpha$  tends to zero. In fact we might investigate more directly  $\mathfrak{D}_k(0)$ . For  $\alpha = 0$  the only  $\mathfrak{D}_k(0)$  are the ones which are nodal partitions associated with  $\lambda_k(0) = L_k(0)$ .

We have investigated this situation for rectangles. We have seen that in this case the nodal partition can only have critical points at the boundary.

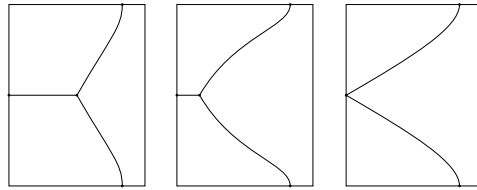


Figure 7. Deformation for type (a).

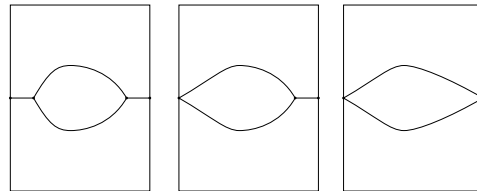


Figure 8. Deformation for type (b).

Let us start with a slightly more general situation and consider a family  $\Omega(\beta)$  of simply connected domains which depends analytically upon a parameter  $\beta \geq 0$ . We assume that the spectrum and eigenfunctions corresponding to  $H(\Omega(\beta))$  have for small  $\beta \geq 0$  the following properties

$$\lambda_1(\beta) < \lambda_2(\beta) < \lambda_3(\beta) \leq \lambda_4(\beta) = L_3(\beta), \tag{7.2}$$

with

$$\lambda_3(\beta) < \lambda_4(\beta) \quad \text{for } \beta > 0 \quad \text{and} \quad \lambda_3(0) = \lambda_4(0). \tag{7.3}$$

Here as usual  $H(\Omega(\beta))$  is just  $-\Delta$  with a Dirichlet boundary condition. We further assume that for  $0 < \beta < \beta_0$ ,  $\mu(u_3(\beta)) = 2$ , but that for  $\beta = 0$  the eigenspace  $U_3$  of  $\lambda_1(0)$  contains an eigenfunction  $u \in U_3$  with  $\mu(u) = 3$ . We hence have for  $\beta > 0$  that  $\lambda_3(\beta)$  is not Courant sharp and therefore there is a  $\mathcal{L}_3(\beta) > \lambda_3(\beta)$ . But for  $\beta = 0$  we have  $\mathcal{L}_3(0) = \lambda_3(0)$ .

According to proposition 2.5 we have for  $\beta > 0$  three types of non-bipartite partitions, (a), (b), (c). But we have observed that for  $\mathcal{L}_3(0)$ , there is no  $\mathfrak{D}_3(0)$  which is not bipartite. So we would like to understand how a non-bipartite partition  $\mathfrak{D}_3(\beta)$  can be deformed so that it becomes bipartite. We emphasize that at the moment we have no mathematical tools permitting us to rigorously prove the validity of these ‘deformation arguments’ but numerical tests show that they are rather good for predicting what is observed.

- (a) If the family is of type (a), what seems natural to imagine (see figure 7) is that the critical point should move to one point of the boundary and that (at least) two lines will start from this point and end at two other points of the boundary. These three points are not necessarily distinct.
- (b) If the family is of type (b), then the two critical points should again tend to the boundary (see figure 8). We note indeed that in the case when  $z_1, z_2$  tend to a point  $z \in \Omega$ , we get four nodal domains.
- (c) In case (c), a new situation can occur when the two critical points tend to one point in  $\Omega$ . One could indeed imagine a deformation of type (c) minimal partitions on a 3-partition which is diffeomorphic to the figure eight (see figure 9).

Let us recall that in the case of the rectangle we have explicitly verified that a limiting minimal partition cannot have a critical point inside the rectangle.

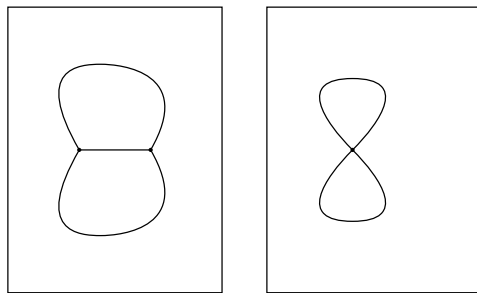


Figure 9. Deformation for type (c).

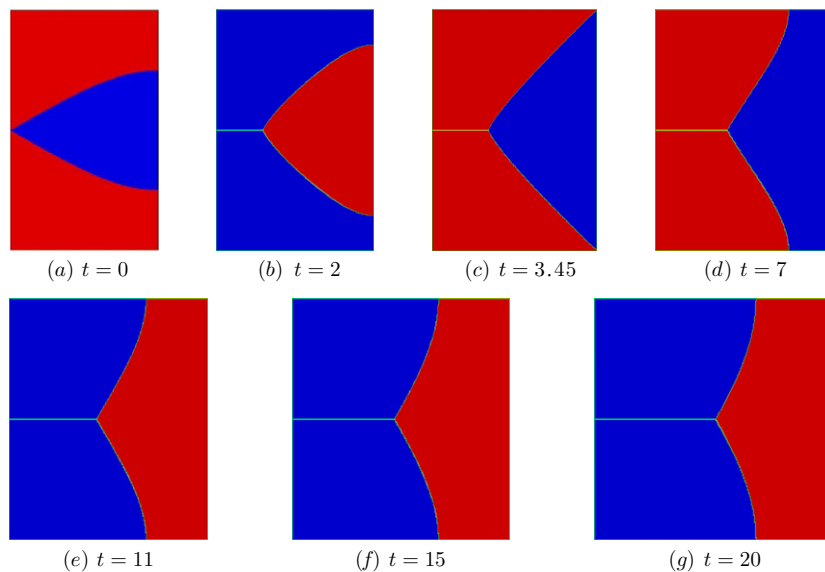


Figure 10. Simulations for rectangles  $\mathbf{R}_{\pi\epsilon,\pi}$  with  $\epsilon = (1 - \frac{t}{20})\sqrt{\frac{3}{8}} + \frac{t}{20}$ .

### 7.2. Numerics for a family of rectangles

We look at the case when the parameter  $\beta$  introduced in the heuristic subsection is the  $\epsilon$  of the computations and we go from  $\epsilon = \sqrt{3/8}$  to  $\epsilon = 1$ . We assume that all the minimal partitions are symmetric with respect to the horizontal axis  $\{y = 0\}$  and of type (a). This permits us to use the argument of reduction to an half-rectangle and to use the approach of the Dirichlet–Neumann for each value of  $\epsilon$ . Figures 10 present the evolution of the candidate to be minimal 3-partition for rectangles  $\mathbf{R}_{\pi\epsilon,\pi}$  with  $\epsilon$  from  $\sqrt{3/8}$  to 1.

As mentioned in [8], numerical simulations on the half-square with mixed condition Dirichlet–Neumann–Dirichlet or Neumann–Dirichlet–Neumann never produce any 3-partitions of type (b) or (c).

## 8. Conclusion

In this paper, we focus on minimal 3-partitions of the rectangle with side lengths  $a, b$ . When  $0 < a/b < \sqrt{3/8}$ , the minimal 3-partition is bipartite and is given by the nodal partition of the

third eigenfunction. It is more complicated as soon as  $a/b \geq \sqrt{3/8}$ . Section 4 concerns the case  $a/b = \sqrt{3/8}$  and we describe a possible mechanism of transition from nodal to non-nodal minimal partition (see figure 3).

In [8, 10], we exhibited two candidates to be the minimal 3-partition for the square. These candidates for the minimal partition lead to the computations of the second eigenfunction of a mixed Dirichlet–Neumann problem on the half-square. According to the considered symmetry, we obtain two candidates (see figures 1(a) and 1(b)). Assuming that the critical point of these candidates is the center of the square, we prove that these candidates yield the same partition energy using arguments of isospectrality and linking the mixed problems with the Aharonov–Bohm Hamiltonians on a punctured domain.

In section 7, we propose a mechanism of transition for the 3-partition of a rectangle to that of the square. Such a question can also be asked for the transition from a thin ellipse to a circle or from a long triangle to an equilateral triangle<sup>12</sup>. One difficulty with these geometries is that the eigenmodes are no more explicit. We can discuss similarly the minimal partitions on angular sectors  $S(\alpha) = \{r \in (0, 1), \theta \in (0, \alpha)\}$  according to  $\alpha$ . For  $\alpha$  small, the minimal 3-partition is nodal and there is a critical value of  $\alpha$  corresponding to the transition to non-nodal 3-partitions.

Using the covering approach mentioned in section 6.3, some numerical simulations have been realized by the first two authors in [9] with two aims. The first one is to exhibit new candidates for the square (and also for any polygons) without any symmetric argument. The second one consists in checking that the critical point of the minimal 3-partition is the center of the square. For this, we compute the 6th eigenfunction of the Dirichlet Laplacian operator on the covering square and we move the interior point of the cutting. Numerical simulations are available on the website (see [10]) <http://w3.bretagne.ens-cachan.fr/math/simulations/MinimalPartitions>.

An analysis of the disc is proposed in [20] and in [21] for the sphere.

Motivated by the partitions mentioned in [16], it seems possible to construct 5-partitions of the square using also symmetric arguments and working with a mixed Dirichlet–Neumann problem in the eighth of the square. The arguments presented here could probably be adapted in this case. In [11], a probabilistic approach leads to some 4- and 5-partitions and describes possible candidates for minimal partitions.

## Acknowledgments

We thank M Van den Berg for indicating to us the existence of [16] and D Mangoubi for mentioning to one of us the recent preprint [25]. We thank also S Terracini for explaining to us the results of her PhD Student B Norris on Aharonov–Bohm Hamiltonians and G Vial for discussion about the numerics. We also thank P Freitas, D Jakobson, M Levitin, L Parnowski, I Polterovich and G Verzini for useful discussions. We also thank the referees for their useful comments.

## References

- [1] Alziary B, Fleckinger-Pellé J and Takáč P 2003 Eigenfunctions and Hardy inequalities for a magnetic Schrödinger operator in  $\mathbb{R}^2$  *Math. Methods Appl. Sci.* **26** 1093–136
- [2] Ancona A, Helffer B and Hoffmann-Ostenhof T 2004 Nodal domain theorems à la Courant *Doc. Math.* **9** 283–99
- [3] Bérard P 1989 Variétés riemanniennes isospectrales non-isométriques *Astérisque* (177-178) Exp. No. 705, 127–54 Séminaire Bourbaki, vol 1988/89

<sup>12</sup> Discussions with P Freitas for the case of the triangle were quite fruitful.

- [4] Bérard P 1992 Transplantation et isospectralité: I *Math. Ann.* **292** 547–59
- [5] Bérard P 1993 Transplantation et isospectralité: II *J. London Math. Soc. (2)* **48** 565–76
- [6] Bérard P and Besson G 1980 Spectres et groupes cristallographiques: II. Domaines sphériques *Ann. Inst. Fourier (Grenoble)* **30** 237–48
- [7] Berger J and Rubinstein J 1999 On the zero set of the wave function in superconductivity *Commun. Math. Phys.* **202** 621–9
- [8] Bonnaillie-Noël V, Helffer B and Vial G 2009 Numerical simulations for nodal domains and spectral minimal partitions *ESAIM Control Optim. Calc. Var.* at press (DOI: [10.1051/cocv:2008074](https://doi.org/10.1051/cocv:2008074))
- [9] Bonnaillie-Noël V and Helffer B 2009 Numerical simulations for minimal partitions with covering approach (in preparation)
- [10] Bonnaillie-Noël V and Vial G 2009 Computations for nodal domains and spectral minimal partitions <http://w3.bretagne.ens-cachan.fr/math/simulations/MinimalPartitions>
- [11] Burdzy K, Holyst R, Ingerman D and March P 1996 Configurational transition in a Fleming–Viot-type model and probabilistic interpretation of Laplacian eigenfunctions *J. Phys. A: Math. Gen.* **29** 2633–42
- [12] Caffarelli L A and Lin F H 2007 An optimal partition problem for eigenvalues *J. Sci. Comput.* **31** 5–18
- [13] Conti M, Terracini S and Verzini G 2003 An optimal partition problem related to nonlinear eigenvalues *J. Funct. Anal.* **198** 160–96
- [14] Conti M, Terracini S and Verzini G 2005 On a class of optimal partition problems related to the Fučík spectrum and to the monotonicity formulae *Calc. Var. Partial Diff. Equ.* **22** 45–72
- [15] Conti M, Terracini S and Verzini G 2005 A variational problem for the spatial segregation of reaction-diffusion systems *Indiana Univ. Math. J.* **54** 779–815
- [16] Cybulski O, Babin V and Holyst R 2005 Minimization of the Rényi entropy production in the space-partitioning process *Phys. Rev. E* **71** 046130
- [17] Helffer B 2007 Domaines nodaux et partitions spectrales minimales (d’après B. Helffer, T. Hoffmann-Ostenhof et S. Terracini) *Sémin. Équ. Dériv. Partielles 2006–2007* Exp. No. VIII, 23. École Polytech., Palaiseau
- [18] Helffer B, Hoffmann-Ostenhof M, Hoffmann-Ostenhof T and Owen M P 1999 Nodal sets for ground states of Schrödinger operators with zero magnetic field in non-simply connected domains *Commun. Math. Phys.* **202** 629–49
- [19] Helffer B, Hoffmann-Ostenhof T and Terracini S 2009 Nodal domains and spectral minimal partitions *Ann. Inst. H. Poincaré Anal. Non Linéaire* **26** 101–38
- [20] Helffer B and Hoffmann-Ostenhof T 2009 On minimal partitions: new properties and applications to the disk *Proc. Conf. Spectrum and Dynamics (June 2008) (CRM Lecture Notes)* to appear
- [21] Helffer B, Hoffmann-Ostenhof T and Terracini S 2009 On spectral minimal partitions: the case of the sphere [arXiv:0903.3326](https://arxiv.org/abs/0903.3326) [math]
- [22] Jakobson D, Levitin M, Nadirashvili N and Polterovich I 2006 Spectral problems with mixed Dirichlet–Neumann boundary conditions: isospectrality and beyond *J. Comput. Appl. Math.* **194** 141–55
- [23] Levitin M, Parnowski L and Polterovich I 2006 Isospectral domains with mixed boundary conditions *J. Phys. A: Math. Gen.* **39** 2073–82
- [24] Pleijel Å 1956 Remarks on Courant’s nodal line theorem *Commun. Pure Appl. Math.* **9** 543–50
- [25] Parzanchevski O and Band R 2008 Linear representations and isospectrality with boundary conditions [arXiv:0806.1042v2](https://arxiv.org/abs/0806.1042v2) [math.SP]
- [26] Sunada T 1985 Riemannian coverings and isospectral manifolds *Ann. Math.* **121** 169–86